Gregorij Kurillo*
University of California, Berkeley
#475 Hearst Memorial Mining Building
Berkeley, CA 94720
and
Faculty of Electrical Engineering
University of Ljubljana
Ljubljana, Slovenia

Matjaž Mihelj
Marko Munih
Tadej Bajd
Faculty of Electrical Engineering
University of Ljubljana
Ljubljana, Slovenia

Multi-Fingered Grasping and Manipulation in Virtual Environments Using an Isometric Finger Device

Abstract

In this article we present a new isometric input device for multi-fingered grasping in virtual environments. The device was designed to simultaneously assess forces applied by the thumb, index, and middle finger. A mathematical model of grasping, adopted from the analysis of multi-fingered robot hands, was applied to achieve multi-fingered interaction with virtual objects. We used the concept of visual haptic feedback where the user was presented with visual cues to acquire haptic information from the virtual environment. The virtual object corresponded dynamically to the forces and torques applied by the three fingers. The application of the isometric finger device for multi-fingered interaction is demonstrated in four tasks aimed at the rehabilitation of hand function in stroke patients. The tasks include opening the combination lock on a safe, filling and pouring water from a glass, muscle strength training with an elastic torus, and a force tracking task. The training tasks were designed to train patients' grip force coordination and increase muscle strength through repetitive exercises. The presented virtual reality system was evaluated in a group of healthy subjects and two post-stroke patients (early post-stroke and chronic) to obtain overall performance results. The healthy subjects demonstrated consistent performance with the finger device after the first few trials. The two post-stroke patients completed all four tasks, however, with much lower performance scores as compared to healthy subjects. The results of the preliminary assessment suggest that the patients could further improve their performance through virtual reality training.

1 Introduction

Interaction with objects in a virtual environment (VE) through grasping and manipulation is an important feature of future virtual reality simulations (Boud, Baber, & Steiner, 1998). Hand manipulation is possible by pushing, pulling, or grasping the object to change its position, orientation, or shape (i.e., deformation). Realistic grasping in a VE is achieved through accurate modeling of forces and torques resulting from the fingertips in contact with the surface of the virtual object. The model of multi-fingered grasping can be adopted from the analysis of multi-fingered robotic hands (Murray, Li, & Sastry, 1994; Montana, 1995) to appropriately describe the effects of whole-hand

Presence, *Vol. 16, No. 3, June 2007, 293–306*

*Correspondence to gregorij@eecs.berkeley.edu.

manipulation. Accurate dynamics modeling of multi-fingered grasping can greatly increase the realism of the interaction within the VE.

In many VE applications, data gloves are used to manipulate and interact with virtual objects. These gloves provide information on the position of the fingers while no data on grasping forces are collected. The user relies only on visual feedback to obtain information on the state of the manipulated object (Boulic, Rezzonico, & Thalmann, 1996). During manipulation in a real environment, proprioceptive and tactile feedback is received through the human sensing system providing information on the grasping force and collision with different objects (Jones, 1997; Lok, Naik, Whitton, & Brooks, 2003). Interaction with data gloves can be further enhanced by using a haptic interface which provides active force feedback to the user in addition to the visual feedback provided by the virtual reality application. Whole-hand haptic systems must offer a high level of mobility of the fingers and haptic feedback in different areas of the hand (Tzafestas, 2003). Several haptic devices have been proposed for multi-fingered interaction in VEs. Bouzit, Burdea, Popescu, and Boian (2002) designed the Rutgers Master II with a pneumatic-driven actuator platform which provides force feedback to the fingers. Zaeh, Egermeier, Petzold, and Spitzweg (2004) used the CyberGrasp commercial exoskeleton device with the CyberGlove data glove (both systems by Immersion Corporation, San Jose, CA) for multi-fingered manipulation of objects in VE. The whole-hand haptic interface devices often require complex control algorithms (Kawasaki, Takai, & Tanaka, 2003) and provide relatively small feedback forces while allowing movement in only limited degrees of freedom. Haptic feedback can be partially replaced by a low-cost alternative such as visual force feedback (Richard, Burdea, Gomez, & Coiffet, 1994; Boud et al., 1998; Burns et al., 2005) where haptic information is presented to the user through visual cues. Compared to data gloves, where the motion of the fingers is unconstrained, the passive haptic devices constrain the motion while measuring the force applied to the force sensing elements (Pai, VanDerLoo, Sadhukhan, & Kry, 2005). If the visual feedback requires an increase of the input force, the user will apply additional force and consequently feel larger resistance at the fingertips, creating in this way the illusion of tactile feedback (Lécuyer, Coquillart, Kheddar, Richard, & Coiffet, 2000). Several isometric devices have been proposed for interaction with VEs. Zhai (1998) presented Fingerball which incorporates a ball-shaped interface with passive force feedback experienced during manipulation. An isometric haptic device, DigiHaptic, presented by Casiez, Plénacoste, Chaillou, and Semail (2003) allows three-fingered interaction with virtual objects. Each of the three fingers is used independently to control one degree of freedom. Pai and colleagues (2005) presented a passive haptic interface Tango intended for whole-hand interaction with 3D objects. The ball-shaped device is equipped with pressure sensors to allow detection of finger positions and accelerometers to assess the position and orientation of the device.

In this article we present a new isometric device which was used as an interface for multi-fingered grasping and manipulation in the VEs intended for rehabilitation of post-stroke patients. The device was designed to accurately assess the fingertip forces and torques of three fingers used to interact with virtual objects. Virtual reality enhanced rehabilitation allows training through augmented feedback while using controlled synthetic environments (Holden & Dyar, 2002; Castelnuovo, Lo Priore, Liccione, & Cioffi, 2003). Previous studies have shown beneficial effects of such training in rehabilitation and skill enhancement of the upper extremities (Jack et al., 2001; Holden & Dyar, 2002). In stroke patients, the ability to control and scale grip forces is greatly reduced (Hermsdörfer, Hagl, Nowak, & Marquardt, 2003). The repetition of different motor tasks can initiate the relearning process inside the central nervous system and contribute to the improvement of functionality of the affected muscles (Popović, Popović, & Sinkjær, 2002). Muscular strength and force control can be also enhanced by isometric training (Kriz, Hermsdörfer, Marquardt, & Mai, 1995; Kurillo, Gregorč, Goljar, & Bajd, 2005). The difficulty level of virtual reality tasks for training can be adjusted to always maximize the patient's performance. With an isometric input, the patient needs very low functional force to accomplish a task. Other advantages of the isometric devices are lower fa-

tigue factor (Zhai, 1998), better safety, and ease of use by patients.

In this article we present the concept of multi-fingered grasping and describe four different VE tasks aimed at improving finger force coordination in stroke patients. The performance of the tasks was evaluated in a group of healthy subjects and two post-stroke patients. We selected the patients at two different stages of post-stroke recovery to assess the effect of their condition on the performance in VE.

2 Isometric Finger Device

The isometric finger device was designed to simultaneously measure forces and torques applied by the thumb, index, and middle finger. The device consists of three 3D force-torque measuring sensors (50M31A-125; JR3, Inc., Woodland, California) positioned close to the fingertips (Figure 1). The sensors are mounted on the aluminum assembly, which provides firm support for the sensors during the measurement. The measurement range of the sensors is ±150 N for the lateral forces and ±300 N for the axial force with a torque range of ±8 Nm. The resolution of the sensors is 0.04 N for the lateral forces, 0.08 N for the axial force, and 0.002 Nm for the torques. The approximate external envelope of the finger device measures 220 × 100 × 160 mm and the total weight is 1.8 kg. During the measurement the hand is positioned between the thumb and the index and middle finger sensors. Finger supports are used to position the fingers in the correct configuration while providing transfer of forces and torques to the sensors. The finger supports are made of acrylic which provides a rigid connection between the fingertip and the sensor. The shape of the finger support was designed considering anthropometric and ergonomic factors. The fingers are fastened to the support using Velcro straps. The distance between the thumb and the two fingers is set at 65 mm to provide a comfortable position for the hand. A forearm support can be used to stabilize the patient's arm and to keep the wrist in a neutral position. The device can be applied for either left or right hand measurement by changing the orientation of the sensor platform by 180°. The data from the three sensors is acquired through a PCI receiver-processor board with a maximal sampling frequency of 500 Hz. The data are filtered in real time by an onboard integrated filter with a cutoff frequency of 32.25 Hz and a time delay of approximately 32 ms.

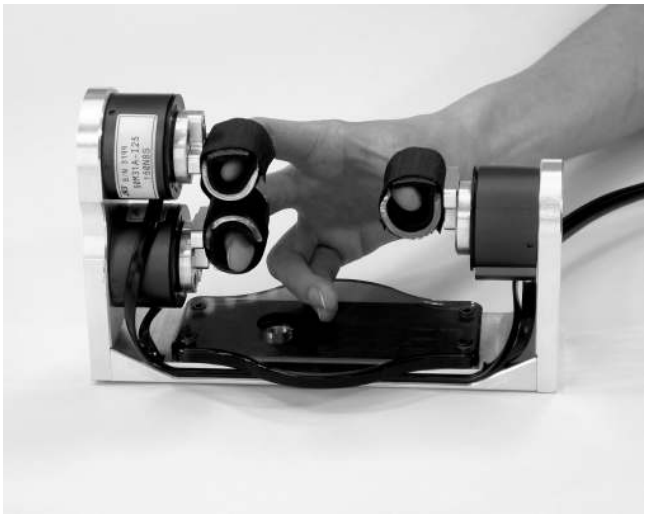

Figure 1. *Isometric finger device enabling the input of fingertip forces for multi-fingered grasping in virtual environments.*

3 Model of Grasping in VE

3.1 Mathematical Model of Grasping

To describe multi-fingered manipulation of an object, a mapping between the fingertip forces and the resultant wrench (i.e., three force and three torque components) on the object, with regard to its center of mass, is needed. Grasping in the VE can be described using a similar approach as used for multi-fingered robotic hands (Murray et al., 1994). In our model of grasping, we assume that the location of the fingers, when in contact with the object, is fixed relative to its center of mass. This assumption is comparable to grasping real objects when the position of the fingers remains constant during manipulation (e.g., lifting an object from a table). The location of the ith contact point in our model (Figure 2) is defined by the coordinate sys-

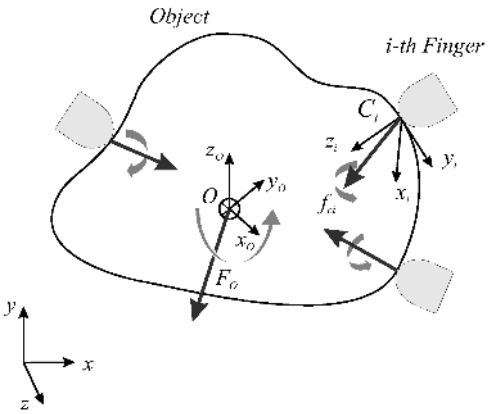

Figure 2. *Kinematic model of grasping a virtual object with multiple rigid fingers.*

tem C_i with the z-axis pointing inwards to the object surface. The position and orientation of the contact coordinate system are described by the vector $\boldsymbol{p}_{oci} \in \Re^3$ and the rotational matrix $\boldsymbol{R}_{oci} \in \Re^{3\times3}$, respectively. The force applied at the contact point is defined by the contact wrench $\boldsymbol{F}_{Ci} \in \Re^6$ consisting of the force and torque vectors of the corresponding fingertip. Two contact types were implemented in our model: point contact with friction and soft finger contact (Montana, 1995). The type of contact is described by the corresponding wrench basis $\boldsymbol{B}_{Ci} \in \Re^{6\times p}$ which defines the number of degrees of freedom p in which the object is fully constrained by the finger. In the case of point contact with friction, the contact wrench with respect to the corresponding wrench basis is described as follows:

$$\boldsymbol{F}_{C_i} = \boldsymbol{B}_{C_i} \cdot \boldsymbol{f}_{C_i} = \begin{bmatrix} 1 & 0 & 0 & 0 & 0 & 0 \\ 0 & 1 & 0 & 0 & 0 & 0 \\ 0 & 0 & 1 & 0 & 0 & 0 \end{bmatrix}^{\mathrm{T}} \cdot \boldsymbol{f}_{C_i} \qquad (1)$$

The vector $\boldsymbol{f}_{Ci} \in \Re^p$ describes the forces and torques applied by the fingers which correspond to the selected friction model. A Coulomb friction model was employed in which the normal force was defined to be positive and the lateral forces proportional to the applied normal force.

The transformation of the fingertip forces of multiple (k) contacts into the resulting wrench on the object, with respect to the center of mass, is described by the grasp map $\boldsymbol{G} \in \Re^{6\times kp}$. The contact wrench $\boldsymbol{f}_{Ci}$ of the ith finger is transformed to the object coordinate system using the contact map $\boldsymbol{G}_i \in \Re^{6\times p}$:

$$\boldsymbol{F}_{OC_i} = \begin{bmatrix} \boldsymbol{R}_{OC_i} & 0 \\ \boldsymbol{P}_{OC_i} & \boldsymbol{R}_{OC_i} \end{bmatrix} \cdot \boldsymbol{B}_{C_i} \cdot \boldsymbol{f}_{C_i} = \boldsymbol{G}_i \cdot \boldsymbol{f}_{C_i} \qquad (2)$$

The matrix $\boldsymbol{P}_{OCi}$ represents the antisymmetrical matrix of the vector $\boldsymbol{p}_{OCi}$ describing the position of the contact point. The resulting wrench of k fingers is described by the sum of contributions from all the contact points:

$$\begin{aligned} \boldsymbol{F}_O &= \boldsymbol{G}_1 \cdot \boldsymbol{f}_{C_1} + \boldsymbol{G}_2 \cdot \boldsymbol{f}_{C_2} + \cdots + \boldsymbol{G}_k \cdot \boldsymbol{f}_{C_k} \\ &= [\boldsymbol{G}_1 \cdots \boldsymbol{G}_k] \cdot [\boldsymbol{f}_{C_1} \cdots \boldsymbol{f}_{C_k}]^{\mathrm{T}} \end{aligned} \qquad (3)$$

Finally, the contact maps $\boldsymbol{G}_i$ of each contact point are collected in the grasp map, defined as matrix $\boldsymbol{G}$:

$$\boldsymbol{F}_O = \boldsymbol{G} \cdot \boldsymbol{f}_C \qquad (4)$$

Equation (4) defines the transformation of matrix of the fingertip forces $\boldsymbol{f}_C \in \Re^{kp}$ into the resulting force and torque on the object defined as the wrench vector $\boldsymbol{F}_O \in \Re^6$.

3.2 Mathematical Model of Object Dynamics

For realistic interaction with an object in a virtual environment, a mathematical model of body dynamics is needed. The model describes dynamic behavior of the object influenced by the fingertip forces and other external forces (e.g., friction, gravity) or torques. In the model, the object motion is constrained by stiffness and friction in all six degrees of freedom (i.e., three translations and three rotations), which are illustrated as virtual springs and dampers in Figure 3. Dynamic behavior of the object is controlled by adjusting the stiffness and friction parameters. With high stiffness of the virtual spring and sufficient friction, the speed of movement in the selected direction can be directly proportional to the input force. With low stiffness of the virtual spring and low friction, the object will behave as if it is attached to a real spring. The parameters can be adjusted according to the application. The number of active degrees of freedom can be limited in a particular direction (e.g., a

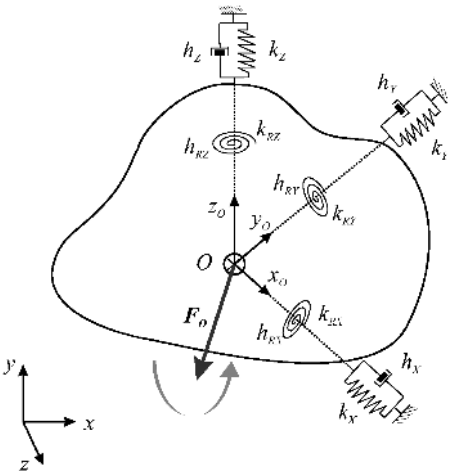

Figure 3. *Object dynamics is modeled using virtual stiffness (k_i) and friction (h_i) in all six degrees of freedom.*

knob must only rotate around its main axis; the other five degrees of freedom are constrained). The dynamic model of the object incorporates object mass, inertia, basic shape (e.g., sphere, cylinder), and location of its center of mass. The environment variables include stiffness of the virtual springs and their viscous friction (Figure 3).

To describe body dynamics in the local coordinates, we used Newton-Euler equations written in the matrix form as follows (Sciavicco & Siciliano, 2002):

$$\boldsymbol{M}\cdot\ddot{\boldsymbol{x}} + \boldsymbol{C}\cdot\dot{\boldsymbol{x}} + \boldsymbol{N}\cdot\boldsymbol{x} + \boldsymbol{g} = \boldsymbol{F_O} \qquad (5)$$

In Eq. (5) $\boldsymbol{x} \in \Re^6$ represents the vector of local coordinates describing the object pose (three parameters for position and roll-pitch-yaw parameters for orientation), the matrix $\boldsymbol{M} \in \Re^{6\times6}$ is the inertia matrix consisting of object mass and inertia parameters, $\boldsymbol{C} \in \Re^{6\times6}$ is a diagonal matrix of friction coefficients, $\boldsymbol{N} \in \Re^{6\times6}$ is a diagonal matrix of stiffness coefficients, and $\boldsymbol{g} \in \Re^6$ is the gravity vector. $\boldsymbol{F_O}$ is the total wrench on the object derived from Eq. (4) of the model for multi-fingered grasping. In our environment, gravity was excluded from the model since it would be too difficult to compensate for using the isometric input. In the case of active gravity, the user would have to continuously apply a force in the vertical direction to keep the object from falling, which would be especially difficult for patients with reduced motor control.

Next the acceleration vector is expressed from Eq. (5):

$$\ddot{\boldsymbol{x}} = \boldsymbol{M}^{-1}(\boldsymbol{F_O} - \boldsymbol{C}\cdot\dot{\boldsymbol{x}} - \boldsymbol{N}\cdot\boldsymbol{x}) \qquad (6)$$

To obtain the position and orientation of the object in local coordinates, Euler integration is used on Eq. (6):

$$\boldsymbol{x} = \iint \ddot{\boldsymbol{x}}\cdot dt = \iint \boldsymbol{M}^{-1}(\boldsymbol{F_O} - \boldsymbol{C}\cdot\dot{\boldsymbol{x}} - \boldsymbol{N}\cdot\boldsymbol{x})\cdot dt \qquad (7)$$

Equation (7) describes the dynamic behavior of the virtual object in space and time resulting from the total wrench on the object, its physical properties, and given environmental variables.

3.3 Grasping in Virtual Environment

The visualization of our VEs was achieved using an open source virtual reality system MAVERIK (Advanced Interfaces Group, School of Computer Science, The University of Manchester, UK), which is based on the OpenGL graphics library (Hubbold et al., 2001). Two additional C libraries were programmed to include the mathematical models of the environment and grasping independent of the visualization engine. The rendering loop allows the update of visualization with 60 frames per second while the data acquisition loop for the measurement of the fingertip forces runs with the frequency of 100 Hz.

The finger device allows only isometric measurements with no movement; therefore, the position of the contact points would be difficult to control. The positions of the virtual fingers are fixed relative to the object and shown on the screen as simplified cone-shaped fingertips. A threshold force must be exceeded for the virtual fingers to come in contact with the object. The virtual fingers are moved along the main axis proportional to the applied force until the collision with the object is detected. If the force of an individual finger is below the threshold, the contact is inactive and does not influence the total wrench on the object. When the threshold is

exceeded and contact with the object is made, the color of the individual virtual finger is changed from red to green, signaling activation of the contact. With one finger in contact, the object can be pushed in the direction of the active fingertip force. The object can be grasped when two or three fingers in opposition are in contact with the object. The total force and torque on the object are determined from the kinematics model of grasping described by Eq. (4) in the previous section. The dynamics of the object are defined by Eq. (6) describing the effect of the resulting force and torque produced by the fingers. Constraints can be implemented to restrict movement in selected directions. Dynamic behavior of the object is controlled for each degree of freedom by changing the stiffness and friction of the virtual springs and dampers.

4 Training Tasks in VE

The virtual reality training application consists of four tasks aimed at assessing and promoting grip force control, finger coordination, and grip strength through repetitive exercises. Each of the four tasks implements the grasping model in connection with the finger device. The virtual rooms were designed to give a realistic impression of grasping while minimizing the complexity of perception.

4.1 Task 1: Open the Safe

In the first task the user is required to open a safe by providing the correct combination (Figure 4, top). The combination code is shown on the screen and the user has to sequentially rotate the knob to find the corresponding symbol. The code is randomly generated in each session. The knob is marked with numbers from 1 to 7 on the right side and letters from A to G on the left side. The neutral position of the knob is denoted with 0. When the knob is turned to match the symbol, the current symbol of the combination code disappears and the user has to find the next character. The user has to first grasp the knob by applying force in the axial direction and then applying torque about the knob axis to turn it to the correct orientation. The knob is connected to a virtual spring and friction which define the dynamics of rotation. The task is completed when the full combination code is provided and the safe is opened.

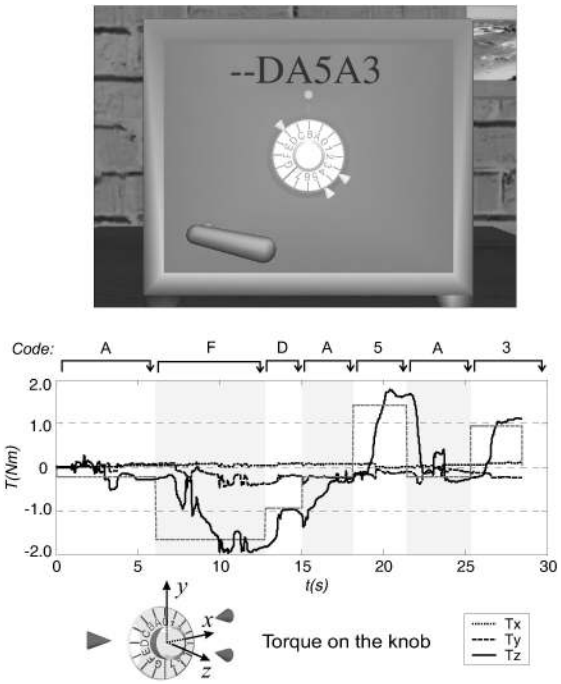

Figure 4. *Task 1: Open the safe (top). The combination of the safe is provided on the screen while the user has to apply appropriate torque to the knob (bottom) to find each symbol of the code. The rotation of the knob is proportional to the applied torque around the z-axis. The corresponding torque values of the presented safe combination are shown with a dashed reference line.*

The difficulty of the task can be modified by changing the length of the code and the maximal torque needed to rotate the knob for the full rotation. Figure 4, bottom, shows the total torque exerted by the healthy subject on the knob while opening the safe. The highest torque is applied around the rotational axis of the knob while the torque around the other two axes is much lower.

The dashed reference line in Figure 4 shows the torque required to open the safe with the shown combination. The reference torque values are proportional to the orientation of the knob for each character of the

code as shown above the chart (e.g., character D corresponds to the torque of −0.95 Nm). The maximal required torque to rotate the knob to letter G was 2 Nm. The orientation tolerance for positioning the knob was set at ±10° and the minimum time delay to provide each symbol was 2 s. The analysis of the reference and exerted torque can provide information on performance accuracy and the time needed to complete the task.

4.2 Task 2: Fill the Jar

In the second task the user has to fill an empty jar with water (Figure 5, top). The task requires the user to grasp the glass, fill it with water from the kitchen faucet, and then pour the water into the jar. The glass is grasped by applying an opposing force with two or three fingers. The glass can be moved in either direction by applying a net force into the corresponding direction while the object is securely grasped. The movement is restricted to the *xy* (vertical) plane and rotation is allowed only normal to this plane.

The low stiffness of the virtual springs with a high level of friction for translational movement allows for an immediate response of the glass position to the applied force. These parameters were adjusted in such a way as to prevent the object position from oscillating when a force is applied or the object is released. When no net force is exerted, the glass would, over a long time period, slowly drift to the initial position due to the limited stiffness and friction. Basic collision detection with bounding boxes is implemented.

The dynamics of water inside the glass corresponds to the motion of the glass. If the water is spilled over the edge of the glass, a water flow is rendered and the volume of water is reduced correspondingly. The task is completed when the water in the jar reaches the marked level (Figure 5, top). The difficulty level can be adjusted by changing the dynamic parameters of the glass and by setting different target levels on the jar. Figure 5, bottom, shows the total torque exerted on the glass during one sequence of the task. Shaded areas indicate each segment of the task (i.e., filling, transport, and pouring). Torque around the *y*-axis gradually increases when pouring out the water. The torque fluctuates slightly

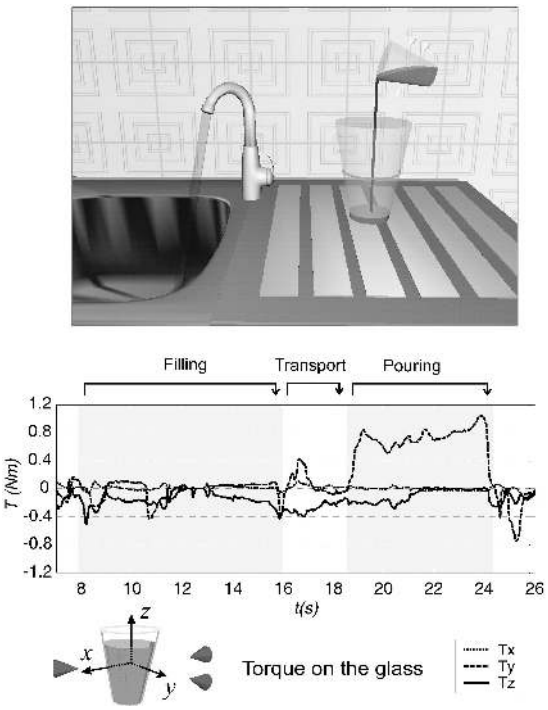

Figure 5. *Task 2: Fill the jar (top). The user is required to grasp the glass, fill it with water, and pour the water into the jar. The output (bottom) shows the applied torques on the glass during the three major segments of the task. Torque around the y-axis is gradually increased during the pouring segment to tilt the glass and fill the jar with water.*

during the filling and transport phase when the subject tries to keep the glass level. The measured fingertip forces can be used to assess the coordination between the fingers during task performance.

4.3 Task 3: Elastic Torus

The third task is aimed at increasing grip strength by repetitive exercises of opening and closing the hand (Figure 6, top). The subject is presented with a deformable torus with geometry and dynamics corresponding to the exerted force between the fingertips. The position of the torus is fixed in space while the elasticity can be adjusted to the abilities of each individual. Global deformation modeling was used to model the elastic torus (Metaxas & Terzopolus, 1992). The user is

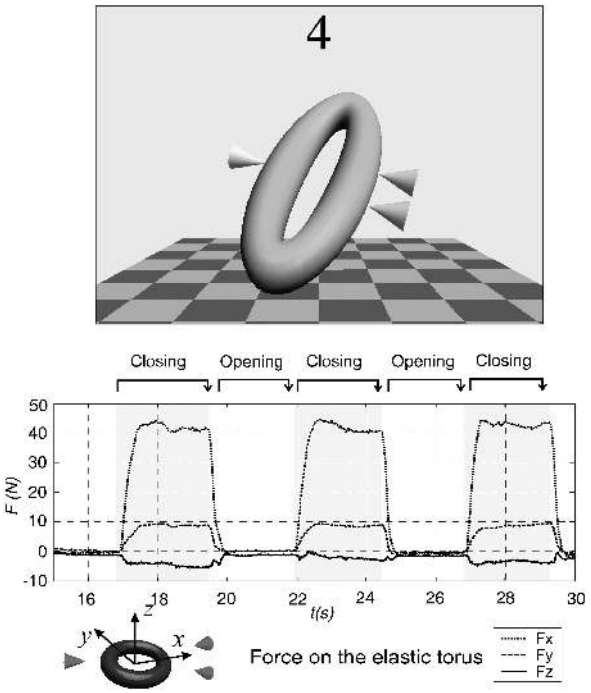

Figure 6. *Task 3: Elastic torus (top). The task is aimed at increasing grip strength by repetitive exercises of hand opening and closing on a deformable torus. The color of the torus changes according to the required action. The output force (bottom) shows an increase of the force in the x- and y-directions, while only a small force was exerted in the z-direction.*

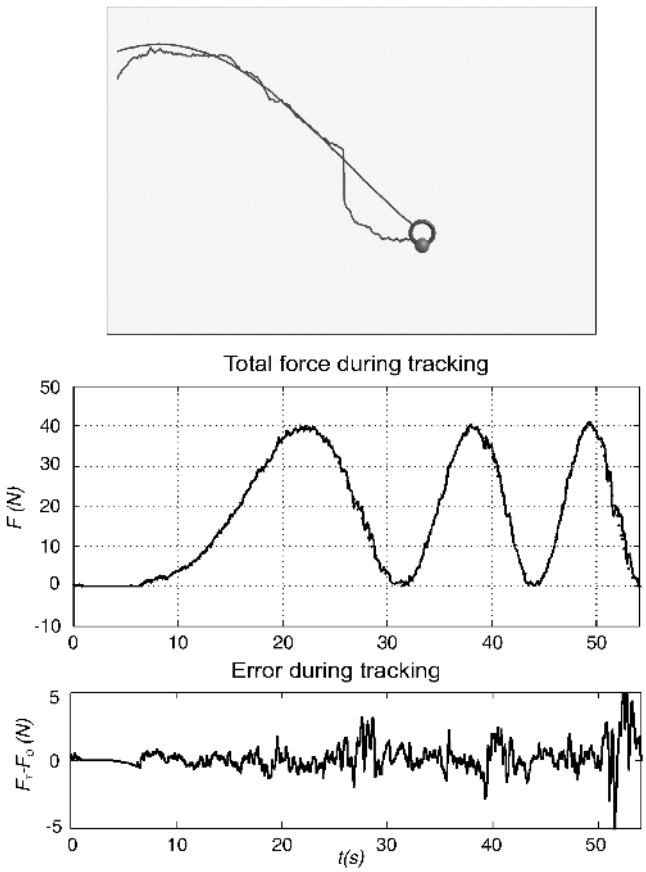

Figure 7. *Task 4: Tracking (top). The tracking task is aimed at the evaluation of grip force control. The user is required to track the presented target signal by simultaneously applying appropriate net force with all three fingers (center). The result of the tracking error (bottom) shows higher accuracy during slow movements of the target as compared to the last segment of the task.*

guided by color cues to correctly perform the exercises. When the torus is compressed beyond the required degree, the color of the object is changed from blue to purple, signaling the user to retain his/her grip. After a specific time period, the color of the torus is changed back to blue, signaling the user to open his/her grip. The counter on the screen shows the number of successfully performed grasping sequences. The difficulty of the task can be adjusted by changing the softness of the torus and the time for each phase. Figure 6, bottom, shows the results of the exerted force on the torus during the task performance as assessed in a healthy person. The highest amplitude of force is exerted in the *x*- and *y*-directions during the compression phase. The healthy subject was able to perform the task rapidly with the final score of 22 sequences per minute. The required minimal force to deform the object was set at 40 N with the minimum time period of 2 s for each sequence. The force results can be used to evaluate grip strength and muscle fatigue during training.

4.4 Task 4: Tracking

The fourth task is intended mainly for the assessment of the overall grip force control (Figure 7, top). The results of previous studies (Kriz et al., 1995; Kurillo et al., 2005) have demonstrated the usefulness of tracking tasks for the training and evaluation of grip force

control. In the tracking task, a person applies force according to visual feedback while trying to minimize the difference between the static or moving target and the actual response. By selecting appropriate dynamic properties and amplitude of the target, the training can be efficiently controlled (e.g., training of the grip release, training of maximal grip force). The difference between the target and measured response can be quantitatively evaluated by the error between the two signals. The target signal is presented with a small blue torus moving vertically in the center of the screen while the applied force response is indicated with a red semi-transparent sphere (Figure 7, top). When the grip force is applied, the red response sphere moves upwards; when the grip is released, the sphere returns to its initial position. The past values of the two signals are presented as two time-varying trails. The abstract nature of the tracking task was chosen with the intention of minimizing the amount of visual information given to the patient during the assessment in order to emphasize motor control rather than visual perception. Figure 7, bottom, shows the output force and error during the tracking task as performed by a healthy subject. The tracking error between the target and the output increases with the rate of the sinusoidal target signal. The peak target force was 40 N. The duration of the task was 60 s. The tracking task results could be used to evaluate improvements in fingertip force coordination during training.

5 Performance Evaluation

The performance of the virtual reality tasks using the finger device was evaluated in a group of 10 healthy subjects with mean age of 27.7 (*SD* 4.2) years and two post-stroke patients. The first patient was a 21-year-old male who suffered a left hemisphere stroke 3 months prior to the testing and was attending regular occupational therapy program. The chronic stroke patient was a 47-year-old male, seven years post left hemisphere stroke, who was considered to be rehabilitated to a large extent. This patient had severe spasticity of the right hand but his overall sensory-motor functions were less affected (e.g., he was able to drive a car). The study was approved by the ethics committee of the Institute for Rehabilitation, Republic of Slovenia.

We first analyzed the overall performance of the VE tasks in the group of healthy subjects. The subjects performed 12 trials for each task in four sessions. The performance of the first and second task was evaluated in terms of the time to successfully complete the task. The third task was evaluated by the number of hand openings and closings during a one minute period. The fourth task was assessed by calculating the relative root mean square error (*rrmse*) between the output force $F_O(t)$ and the sinusoidal target $F_T(t)$ over the trial duration N (Kurillo et al., 2005):

$$rrmse = \sqrt{\frac{1}{N}\sum_{t=0}^{N}\frac{(F_o(t) - F_T(t))^2}{\max(F_T)^2}} \qquad (8)$$

Figure 8 shows the average performance scores in four VR tasks as assessed in healthy subjects. In Task 1 the average time to open the safe was 36.5 s (*SD* 10.2) for the first session (i.e., first three trials) while the average time of the last session (i.e., last three trials) was 26.2 s (*SD* 4.3). The results of Task 2 show the largest improvement in performance after the first few trials. The average time needed to fill up the jar was 70.5 s (*SD* 22.4) in the first session and 42.4 s (*SD* 8.3) in the last session. The results of Task 3 show steady performance in all trials. The average number of hand closing and opening cycles per minute was 22.0 (*SD* 2.0). The results of Task 4 show that the tracking error between the output and the target gradually decreased in the first few trials. The average tracking error of the first session was 0.30 (*SD* 0.05). The subjects improved their performance and decreased their average tracking error to 0.22 (*SD* 0.04) in the last session. In all tasks, the variability in performance among the subjects was much larger at the beginning as compared to the performance assessed after several trials.

Statistical analysis of the performance results between the first and last session examined by *t*-test showed significant improvements in all tasks (Task 1: $t_{58} = 4.88$, $p < .0001$; Task 2: $t_{58} = 5.84$, $p < .0001$; Task 3: $t_{58} = -3.82$, $p < .0003$; Task 4: $t_{58} = 7.11$, $p < .0001$). The results show that the subjects were able

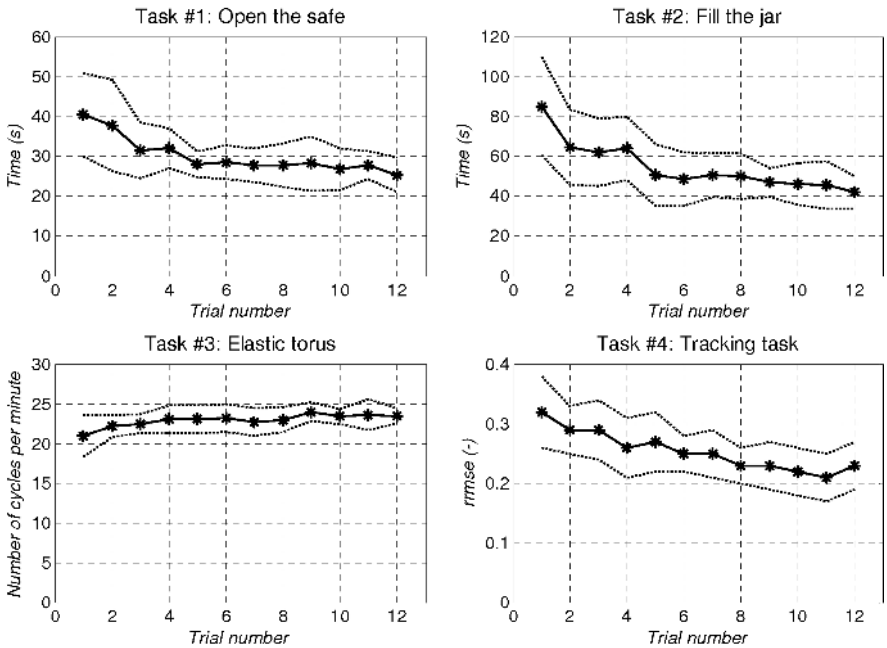

Figure 8. *The average performance scores in four tasks as assessed in the group of ten healthy subjects (dashed lines show standard deviation of mean).*

to quickly learn to manipulate virtual objects using the isometric finger device in the experimental tasks that were tested.

The performance of the VE tasks in the two post-stroke patients was assessed in six sessions. The two patients tried to perform the four tasks with both hands during the initial session. When using the more affected hand, they were able to complete only some of the tasks (Tasks 3 and 4) but the performance was not as consistent due to a high level of spasticity. The patients had difficulty keeping the thumb inside the finger support. The assessment on the more affected hand was therefore discontinued. The patients used their less affected hand to perform the tasks. To reduce fatigue and loss of concentration only one trial of each task was performed per daily session. Figure 9 shows the performance scores as assessed in each task for the less affected hand. The results show significant differences in performance between the patients. The early post-stroke patient was not able to complete Task 2 in the first two sessions but he improved considerably in the subsequent trials (from 1114 s in the third trial to 455 s in the sixth trial). Both patients demonstrated much poorer performance scores as compared to the group of healthy subjects (Figure 8). The chronic post-stroke patient was able to complete Tasks 1 and 4 with scores close to the range of healthy subjects in the last few trials.

The largest difference in performance between the healthy subjects and stroke patients was evident in Task 2 which requires more complex coordination of fingertip forces. Figure 10 shows the position trajectory of the glass as recorded in a healthy subject and two post-stroke patients. The result of the healthy subject shows a smooth trajectory during the transport phase. The subject was able to accurately position the glass during the filling and pouring phase. The position trajectories of the two patients show irregular movement patterns due to reduced sensory-motor control. Both patients had difficulty in simultaneously controlling the position and orientation of the glass during the pouring phase. The early post-stroke patient moved the glass over a much larger area with more abrupt movement patterns than

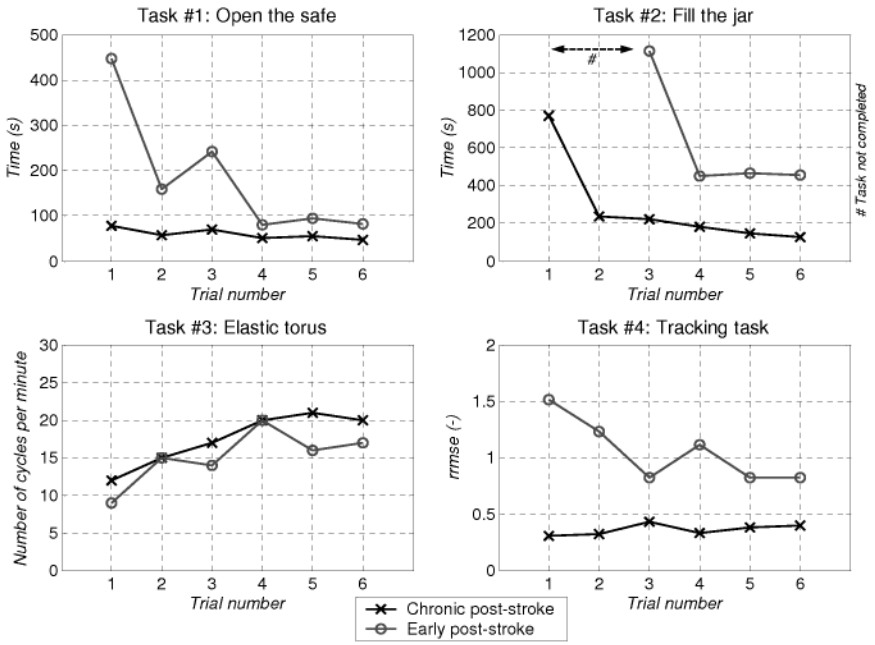

Figure 9. *Performance scores in four tasks as assessed in early and chronic post-stroke patients.*

the chronic post-stroke patient. Similar results can be observed in the other tasks with the two post-stroke patients who produced more abrupt force outputs resulting in lower performance.

6 Conclusions

In this article we presented a new approach to multi-fingered grasping and manipulation in virtual environments using an isometric input device. The finger device developed allows accurate measurement of fingertip forces and torques and provides sufficient information to simulate grasping of objects in a virtual world. The mathematical model of grasping adopted from multi-fingered robotic manipulators was used to transform the fingertip forces into the resulting force and torque on the object. The developed VE grasping library allows simulation of different interaction modes, using only the measured fingertip forces from the isometric finger device. The object can be grasped, pushed,

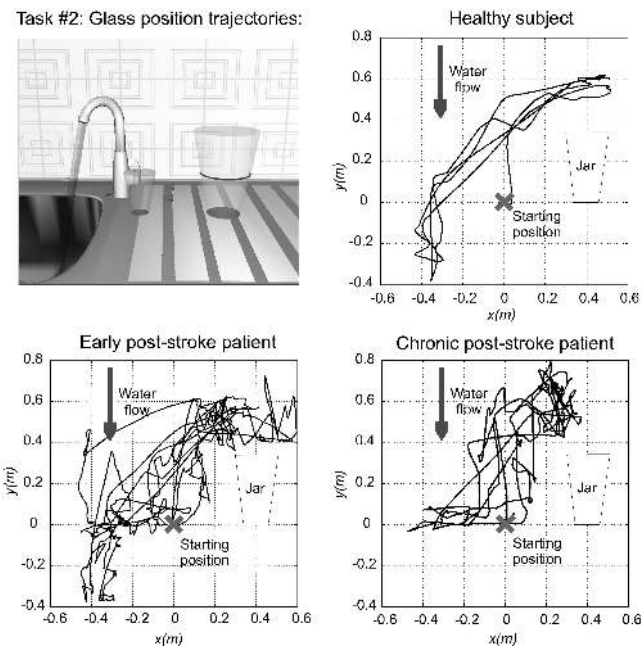

Figure 10. *Position trajectories of the glass as assessed in Task 2 are compared between a healthy subject and two post-stroke patients. Both patients produced irregular movement patterns during performance due to reduced fingertip force control.*

or transported to a new position inside the virtual space with the ability to control the dynamics in each degree of freedom. Although no movement of the fingers is permitted by the finger device, the visual feedback associated with the object dynamics provides sufficient visual cues to simulate the experience of grasping.

In this article, we presented four VEs intended for rehabilitation of hand function after stroke. The tasks are aimed at assessing and promoting grip force control and grip strength through functional activity while being fun and motivating for the patient. The training environments described allow levels of difficulty to be customized to patients' different functional abilities. Only a limited number of degrees of freedom (up to three) were used in each task to reduce the complexity of interaction and to avoid depth perception difficulties. The position of the virtual fingertips was fixed to the object in all tasks. This limitation is comparable to the grasping of real objects when the position of the fingers remains constant during manipulation (i.e., no rolling or sliding of the fingertips is present). By applying a pulling force with a finger (i.e., negative force in the normal direction), the corresponding virtual fingertip would move away from the object and would not contribute to the total force. With this approach the user can see some movement of the fingertip on the screen which, according to subjects' comments, added to the realism of the manipulation experience. The kinematic correspondence of the fingertips is not an issue if the tasks are properly constrained. The manipulation in all the tasks was limited to interaction with a single object. Preliminary testing showed that the complexity of interaction when controlling several degrees of freedom is greatly increased while keeping the object in a firm grip. Limiting the number of degrees of freedom of the object (e.g., restricting the movement to a plane) decreases the complexity of the manipulation task. The accuracy of positioning is sufficient as demonstrated by the overall performance results. Subjects were able to control the orientation of the safe knob within the tolerance limits of $\pm 5°$.

The second task required precise positioning of the glass under the water tap when filling with water or keeping the glass steady above the jar when pouring the water. The results in healthy subjects suggest that rotational movement is easier to control with the finger device than translational movement. An explanation is that wrist rotation to apply torque is more natural than using the wrist for translational movement. In a real environment the arm and wrist are applied in synergy to transport an object from one point to another. The results of the preliminary tests showed that when small forces are required to transport an object, the subjects are able to adapt to this control mode.

The overall performance results in healthy subjects demonstrate that multi-fingered interaction with the finger device is very straightforward. The subjects were able to adapt fairly quickly to the isometric control mode of the virtual fingertips when interacting with virtual objects. The assessment for two post-stroke patients showed that all four tasks can be performed even with sensory-motor function reduced by stroke. These patients had some difficulty controlling the objects with the less affected hand due to excessive or poorly coordinated fingertip forces. The chronic stroke patient performed the tasks much faster and with greater accuracy than the early stroke patient, who was still undergoing occupational therapy. The results suggest that Task 2 could be too complex for some of the early post-stroke patients. Such patients might possibly benefit from the VE training first, using less complex tasks, such as Tasks 3 and 4. During the initial assessment both patients were able to perform these two tasks with the more affected hand but the performance was considerably poor compared to the less affected hand due to the presence of strong spasticity.

Patients with reduced visual-spatial abilities may demonstrate lower performance in more complex virtual environments. The main advantage of using VE for rehabilitation is in the possibility of adjusting the tasks to the individual's sensory-motor and cognitive abilities (e.g., restricting the movement in certain dimensions). Our results show that the post-stroke patients were able to successfully use the isometric finger device to manipulate virtual objects. The patients also showed improvements through each trial.

We believe that the proposed virtual reality system may be used as a supplemental therapy to the standard

rehabilitation exercises. Previous studies have shown that repetitive exercises requiring motor activation with visual feedback can greatly contribute to the reorganization of the damaged central nervous system (Jack et al., 2001; Holden & Dyar, 2002; Popović et al., 2002). In the future, a larger scale clinical study will be performed to assess the effectiveness of the proposed virtual reality system where the patients will be evaluated by the means of standardized clinical measures to follow the progress of therapy.

Further improvements can be made in the design of the hardware to include more cost-efficient sensors. The input device could also be redesigned for specific functional tasks. Use of an isometric input for multi-fingered interaction within the VE provides an alternative to whole-hand (isotonic) haptic devices, especially in the rehabilitation environment. Isometric devices are low-cost, safe, and easy to use and require no lengthy strapping of the patient's hand into a robotic exoskeleton. Both isometric and isotonic training can increase muscle capacity. The isometric devices, however, have a lower fatigue factor (Casiez et al., 2003) and thus offer an alternative in a rehabilitation environment where repetitive tasks are performed. The inherent drawback of isometric input devices is their inability to provide complete haptic position feedback to the user due to the restriction of movement, which may require some initial adaptation to the control mode.

Acknowledgments

The authors would like to thank the volunteers and the patients who participated in this study. The finger device was designed within the ALLADIN project, funded by the European Commission under the 6th Framework Programme, IST Programme, Priority 2.3.1.11—eHealth, IST Contract No. IST-2002-507424. The authors would like to thank the members of the ALLADIN team who in any way contributed to the realization of the finger device. This study was supported by the Ministry of Higher Education, Science and Technology, Republic of Slovenia.

References

Boud, A. C., Baber, C., & Steiner, S. J. (1998). Object manipulation in virtual environments: Effects of visual and haptic feedback. *Proceedings of ICAT' 98,* 124–128.

Boulic, R., Rezzonico, S., & Thalmann, D. (1996). Multi-finger manipulation of virtual objects. *Proceedings of ACM Symposium on Virtual Reality Software and Technology, VRST 96,* 67–74.

Bouzit, M., Burdea, G., Popescu, G., & Boian, R. (2002). The Rutgers Master II—New design force-feedback glove. *IEEE/ASME Transactions on Mechatronics, 7*(2), 256–263.

Burns, E., Razzaque, S., Panter, A. T., Whitton, M. C., McCallus, M. R., & Brooks, F. P. (2005). The hand is slower than the eye: A quantitative exploration of visual dominance over proprioception. *Proceedings of IEEE International Conference on Virtual Reality,* 3–10.

Casiez, G., Plénacoste, P., Chaillou, C., & Semail, B. (2003). The DigiHaptic, a new three degrees of freedom multi-finger haptic device. *Proceedings of Virtual Reality International Conference,* 35–39.

Castelnuovo, G., Lo Priore, C., Liccione, D., & Cioffi, G. (2003). Virtual reality based tools for the rehabilitation of cognitive and executive functions: The V-STORE. *Psychology Journal, 3,* 310–325.

Hermsdörfer, J., Hagl, E., Nowak, D. A., & Marquardt, C. (2003). Grip force control during object manipulation in cerebral stroke. *Clinical Neurophysiology, 114,* 915–929.

Holden, M. K., & Dyar, T. (2002). Virtual environment training: A new tool for neurorehabilitation. *Neurology Report, 26*(2), 62–71.

Hubbold, R., Cook, J., Keats, M., Gibson, S., Howard, T., Murta, A., et al. (2001). GNU/MAVERIK: A microkernel for large-scale virtual environments. *Presence: Teleoperators and Virtual Environments, 10*(1), 22–34.

Jack, D., Boian, R., Merians, A. S., Tremaine, T., Burdea, G. C., Adamovich, S. V., et al. (2001). Virtual reality-enhanced stroke rehabilitation. *IEEE Transactions on Neural Systems and Rehabilitation Engineering, 9*(3), 308–318.

Jones, L. (1997). Dextrous hands: Human, prosthetic and robotic. *Presence: Teleoperators and Virtual Environments, 6*(1), 29–56.

Kawasaki, H., Takai, J., & Tanaka, Y. (2003). Control of multi-fingered haptic interface opposite to human hand. *Proceedings of the 2003 IEEE/RSJ International Conference on Intelligent Robots and Systems,* 2707–2712.

Kriz, G., Hermsdörfer, J., Marquardt, C., & Mai, N. (1995).

Feedback-based training of grip force control in patients with brain damage. *The Archives of Physical Medicine and Rehabilitation, 76,* 653–659.

Kurillo, G., Gregorič, M., Goljar, N., & Bajd, T. (2005). Grip force tracking system for assessment and rehabilitation of hand function. *Technology & Health Care, 13,* 137–149.

Lécuyer, A., Coquillart, S., Kheddar, A., Richard, P., & Coiffet, P. (2000). Pseudo-haptic feedback: Can isometric input devices simulate force feedback? *Proceedings of IEEE International Conference on Virtual Reality,* 83–90.

Lok, B., Naik, S., Whitton, M., & Brooks, F. P. (2003). Effects of handling real objects and self-avatar fidelity on cognitive task performance and sense of presence in virtual environments. *Presence: Teleoperators and Virtual Environments, 12*(6), 615–628.

Metaxas, D., & Terzopolus, D. (1992). Dynamic deformation of solid primitives with constraints. *Proceedings of SIGGRAPH 92,* 309–312.

Montana, D. J. (1995). The kinematics of multi-fingered manipulation. *IEEE Transactions on Robotics and Automation, 11*(4), 491–503.

Murray, R. M., Li, Z., & Sastry, S. S. (1994). *A mathematical introduction to robotic manipulation*. New York: CRC Press.

Pai, D. K., VanDerLoo, E. W., Sadhukhan, S., & Kry, P. G. (2005). The Tango: A tangible tangoreceptive whole-hand human interface. *Proceedings of WorldHaptics,* 141–147.

Popović, D. B., Popović, M. B., & Sinkjær, T. (2002). Neurorehabilitation of upper extremities in humans with sensorymotor impairment. *Neuromodulation, 5*(1), 54–67.

Richard, P., Burdea, G., Gomez, D., & Coiffet, P. (1994). A comparison of haptic, visual and auditive force feedback of deformable virtual objects. *Proceedings of ICAT 94,* 49–62.

Sciavicco, L., & Siciliano, B. (2002). *Modelling and control of robot manipulators*. London: Springer-Verlag.

Tzafestas, C. S. (2003). Whole-hand kinesthetic feedback and haptic perception in dextrous virtual manipulation. *IEEE Transactions on Systems, Man and Cybernetics, Part A, 33*(1), 100–113.

Zaeh, M. F., Egermeier, H., Petzold, B., & Spitzweg, M. (2004). Dexterous object manipulation in a physics based virtual environment. *Proceedings of Mechatronics and Robotics Conference,* 1340–1344.

Zhai, S. (1998). User performance in relation to 3D input device design. *ACM SIGGRAPH Computer Graphics, 32*(4), 50–54.